International Journal of Heat and Mass Transfer 222 (2024) 125202

Contents lists available at ScienceDirect

International Journal of Heat and Mass Transfer

journal homepage: www.elsevier.com/locate/ijhmt

Near-normal nonreciprocal thermal radiation with a 0.3T magnetic field based on double-layer grating structure

Zihe Chen [a], Shilv Yu [a], Cheng Yuan [b], Xiaobing Luo [a], Run Hu [a,*]

[a] School of Energy and Power Engineering, Huazhong University of Science and Technology, Wuhan 430074, China
[b] Wuhan Fiberhome Fuhua Electric Co., Ltd, Wuhan 430074, China

ARTICLE INFO

Keywords:
Nonreciprocal thermal radiation
Moderate magnetic field
Near-normal direction
Double-layer grating

ABSTRACT

The violation of Kirchhoff's law is anticipated to manipulate the emissivity and absorptivity separately and offer new freedom and opportunity for high-efficiency energy harvesting. However, the current designs of nonreciprocal thermal emitters encounter challenges related to large magnetic fields and large incident angles, hindering the practical implementations and applications. This study introduces a novel design involving a metal-SiC grating positioned above a magneto-optical (MO) film, allowing for the generation of robust nonreciprocal thermal radiation in close proximity to the normal direction with a moderate magnetic field of 0.3T. Such magnetic field strength is within the reach of a permanent magnet, which is conducive to practical applications. The manifestation of this phenomenon can be primarily attributed to the guided mode resonance occurring in the low-loss SiC grating, which can enhance the sensitivity to the magnetic field. In addition, the influences of the incident angle and structural dimension parameters on nonreciprocity are also investigated. It is found that this structure can not only realize nonreciprocity at ultra-small angles, but also realize directional nonreciprocal thermal radiation, which greatly expands the applicability of the structure. The present findings remove the limitations of large magnetic field and incident angle for traditional nonreciprocal thermal radiation, and promote the practical realization and application of nonreciprocal thermal emitters.

1. Introduction

Objects with temperatures above absolute zero radiate energy outwardly, and the corresponding spectral properties are described by Plank's law and emissivity. Emissivity refers to the ability of an object to emit radiation and is constrained by Kirchhoff's law, which states that the spectral emissivity and absorptivity are equal for the same direction and frequency [1–3]. When an object absorbs thermal radiation, it simultaneously radiates energy in the same direction. This energy harvesting mechanism hinders efficient recycling of solar energy and significantly reduces energy harvesting efficiency. Thus, if Kirchhoff's law can be violated to enable separate control over the emission and absorption processes, it has the potential to revolutionize the utilization of thermal radiation [4–7].

Traditionally, Kirchhoff's law is a requirement of the Lorentz reciprocity theorem that requires non-magnetic, stationary and linear materials [8,9], resulting in the equal thermal emission and absorption at the same angle (θ) and wavelength (λ). However, the field of photonic engineering has advanced, allowing for the exploration of magnetic response, time-varying systems, and optical nonlinear materials. Consequently, new possibilities have emerged to achieve nonreciprocal thermal radiation. In 2014, Fan's team [3] conducted pioneering research that demonstrated the compatibility of violating Kirchhoff's law with the laws of thermodynamics and presented the first nonreciprocal thermal emitter based on MO materials, enabling nonreciprocal thermal radiation in the mid-infrared and far-infrared ranges when subjected to a large external magnetic field (B). Recently, magnetic Weyl semimetals can achieve strong nonreciprocal thermal radiation without an applied magnetic field [10–13], but this behavior can only be achieved at extremely low temperatures, lacking experimental verification at room temperature [14]. Therefore, most scholars still focus on the design and application of traditional magneto-optical materials. However, the extent of nonreciprocity, characterized by the difference between absorptivity and emissivity, relies on the degree of asymmetry, which is characterized by the ratio of the nondiagonal and diagonal terms of the dielectric tensor [10]. In the case of MO materials, this asymmetry degree is typically around 0.01 within the mid-infrared band, signifying a weak nonreciprocity. Hence, achieving significant

* Corresponding author.
E-mail address: hurun@hust.edu.cn (R. Hu).

https://doi.org/10.1016/j.ijheatmasstransfer.2024.125202
Received 28 September 2023; Received in revised form 9 January 2024; Accepted 13 January 2024
Available online 17 January 2024

nonreciprocity typically necessitates a large magnetic field [3,15–20] or various resonance designs [21–24]. For example, the introduction of a low-loss grating on the MO film to form guided mode resonances achieves the violation of Kirchhoff's law at the wavelength of 25.11 μm with $B = 0.3$ T and θ=65° [21], which has been experimentally verified with a similar structure [25]. Nevertheless, the practical application of nonreciprocal thermal emitters is still hindered by the limitation of a large incident angle. According to Lambert's cosine theorem, the surface radiation intensity is directly proportional to the cosine of the incident angle [22]. Therefore, to achieve optimal energy collection, it is necessary to minimize the angle between the incident light and the device's normal. Despite significant efforts dedicated to nonreciprocal thermal radiation, most existing designs of nonreciprocal thermal emitters often require a large angle, which fails to meet the practical energy application requirements. More recently, some studies have achieved nonreciprocal thermal radiation with θ=1°, but the required magnetic field is mostly above 1T [22,24,26]. Thus, it is crucial to develop a structure that not only enables nonreciprocal thermal radiation at nearly 0° but also requires a lower applied magnetic field.

Here, a novel structure comprising a metal-SiC dielectric grating above the InAs film has been proposed to fulfill the requirements of ultra-small angles and moderate magnetic fields. This design successfully achieves strong nonreciprocal thermal radiation at the wavelength of 23.145 μm with $B = 0.3$ T and θ=1° To uncover the underlying physical mechanism, the distribution of magnetic field amplitude is calculated and analyzed. Furthermore, the impacts of incident angles and structural parameters on nonreciprocal thermal radiation are also explored. The successful realization of this research is expected to greatly contribute to the practical application of nonreciprocal thermal radiation.

2. Method and design

The specific structure employed in this work is illustrated in Fig. 1 (a). It comprises four different materials: SiO_2, SiC, InAs, and metal Al. The top grating structure consists of Al and SiC with a low dielectric loss. The MO material InAs, which exhibits nonreciprocal behavior, is positioned at the bottom of the grating. To ensure the structure acts as a reflector and does not allow transmission, a layer of metal Al serves as the metallic reflector, while SiO_2 serves as the substrate. The specific size parameters are indicated in Fig. 1(a), where the grating period is denoted as p and the grating width as w. Furthermore, from top to bottom, the thicknesses of each part of the structure are h_1, h_2, h_3, h_4, and h_5 respectively.

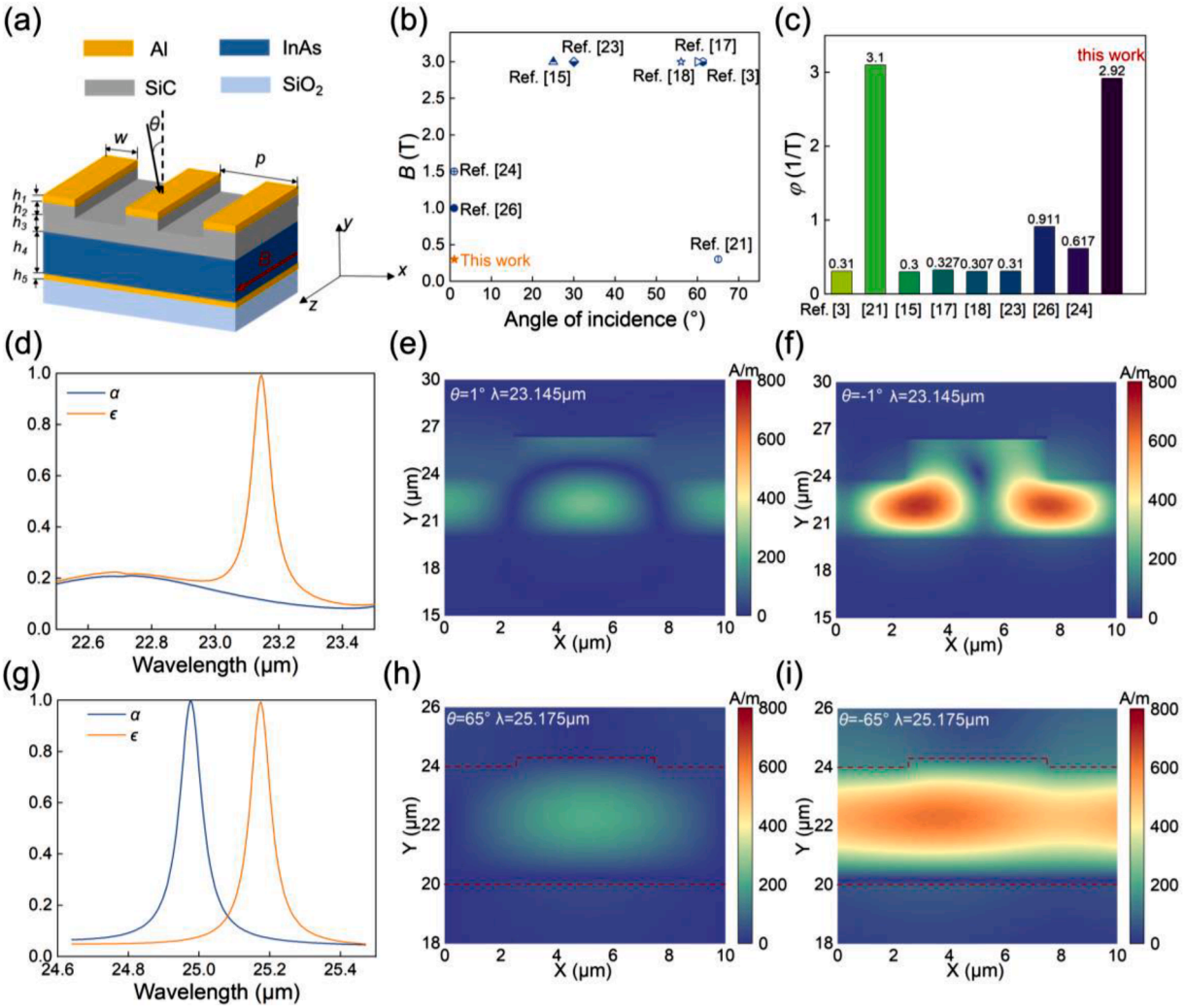

Fig. 1. Near-normal nonreciprocal thermal radiation of MO structure with $B = 0.3$ T: (a) Schematic of the grating structure; (b) Comparison chart with other designs [3,15,17,18,21,23,24,26]; (c) Comparison of φ values between other designs and this work; (d) The absorptivity and emissivity spectra with $B = 0.3$T and $\theta = 1°$; (e) The magnetic field distribution at the wavelength of 23.145 μm with $\theta = 1°$; (f) The magnetic field distribution at the wavelength of 23.145 μm with $\theta = -1°$ The reproduction results of Ref. [21]: (g) The absorptivity and emissivity spectra with $B = 0.3$T and $\theta = 65°$; (h) The magnetic field distribution at the wavelength of 25.175 μm with $\theta = 65°$; (i) The magnetic field distribution at the wavelength of 25.175 μm with $\theta = -65°$

Considering that the external magnetic field is along the z axis, in this case, the dielectric tensor of the MO material InAs is asymmetric and the specific expression is [3]

$$\varepsilon = \begin{bmatrix} \varepsilon_{xx} & \varepsilon_{xy} & 0 \\ \varepsilon_{yx} & \varepsilon_{yy} & 0 \\ 0 & 0 & \varepsilon_{zz} \end{bmatrix} \tag{1}$$

where

$$\varepsilon_{xx} = \varepsilon_{yy} = \varepsilon_{\infty} - \frac{\omega_p^2(\omega + i\Gamma)}{\omega\left[(\omega + i\Gamma)^2 - \omega_c^2\right]} \tag{2}$$

$$\varepsilon_{xy} = -\varepsilon_{yx} = i\frac{\omega_p^2\omega_c}{\omega\left[(\omega + i\Gamma)^2 - \omega_c^2\right]} \tag{3}$$

$$\varepsilon_{zz} = \varepsilon_{\infty} - \frac{\omega_p^2}{\omega(\omega + i\Gamma)} \tag{4}$$

In the above equations, the parameters ε_{∞}, ω_p, ω_c and Γ represent the high-frequency permittivity, the plasma frequency, the cyclotron frequency and the relaxation rate, respectively. Among them, $\varepsilon_{\infty} = 12.37$, $\omega_p = \sqrt{ne^2/(m^*\varepsilon_0)}$, $\omega_c = eB/m^*$, and $\Gamma = 1.55 \times 10^{11}$ rad/s. Here, $n = 7.8 \times 10^{17}\mathrm{cm}^{-3}$ is the free electron carrier density, e is the elementary charge, $m^* = 0.033m_e$ (m_e is the electron mass) is the effective electron mass, ε_0 is the vacuum permittivity and $B = 0.3$T is the external magnetic field. In addition, the permittivity of Al is determined by Drude model and the permittivity of SiC is described by a Lorentz model. The corresponding parameters and definitions can be found in Ref. [21].

Considering that the incident wave is TM wave in the x-y plane with an incident angle θ, the spectral directional absorptivity and emissivity can be determined by calculating the reflectance and transmittance. In this case, we assume that the incident light is fully reflected at the bottom metal, hence neglecting the transmission process. As a result, the expressions for absorptivity α and emissivity ϵ are derived as follows [3, 21]:

$$\alpha(\theta, \lambda) = 1 - R(\theta, \lambda) \tag{5}$$

$$\epsilon(\theta, \lambda) = 1 - R(-\theta, \lambda) \tag{6}$$

Here, R is the spectral reflectivity and the whole calculation results can be obtained by COMSOL Multiphysics.

3. Results and discussion

Firstly, to enhance the nonreciprocal effect, the sizes of the structure are carefully optimized, resulting in the following set of optimized parameters: $p = 10$ μm, $w = 5.1$ μm, h_1=0.24 μm, h_2=2.51 μm, h_3=3.84 μm, h_4=20 μm, h_5=0.2 μm. At an incident angle of 1° and a magnetic field strength of 0.3 T, the corresponding absorptivity and emissivity spectra are depicted in Fig. 1(d). It can be seen that the emissivity reaches 0.993 while the absorptivity is only 0.117 at the wavelength of 23.145 μm, indicating a pronounced violation of Kirchhoff's law. To explain the mechanism behind this phenomenon, the magnetic field distributions with θ=1° and θ=−1° at the wavelength of 23.145 μm have been calculated in Fig. 1(e) and (f). When the incidence angle is −1°, as shown in Fig. 1(f), the magnetic field amplitude in the SiC region is obviously enhanced and shows a stationary wave pattern along the X direction, which represents a typical guided-mode resonance. A stronger magnetic field amplitude results in a higher absorptivity of this structure with θ=−1°, which is corresponded to a higher emissivity with θ=1° In contrast, as shown in Fig. 1(e), the magnetic field amplitude is weak with θ=1° and thus leads to a low absorptivity. Here, in order to better show the differences between this work and the design of Ref. [21], the reproduction results are shown in Fig. 1 (g-i). The absorptivity and emissivity spectra are shown in Fig. 1(g) and the position of the emission peak is slightly shifted within the allowable range. The peak wavelength of the emission in the Ref. [21] is 25.11 μm, and the reproduced result is 25.175 μm. The magnetic field distributions with $\theta = 65°$ and $\theta = -65°$ at the resonant wavelength of 25.175 μm have been calculated in Fig. 1 (h) and (i). Compared with the results of the Ref. [21], the magnetic field distribution in this work has better standing wave distribution characteristics, making it easier to realize guided mode resonance at small angles. Therefore, although the structure designed in this work is similar to that in Ref. [21], our optimized structure is able to achieve nonreciprocal thermal radiation close to the normal direction.

Here, for the purpose of highlighting the superiority of this work, a comparison is made with previous researches, as depicted in Fig. 1(b). Typically, the existing designs operate at large incident angles ranging from 25° to 70° and necessitate a large magnetic field strength of 3 T. Additionally, when the incident angle is 1°, our design only requires a magnetic field strength of 0.3 T, while other works often demand more than 1 T, making our approach more practical and feasible. Moreover, a parameter φ is introduced to characterize the sensitivity of nonreciprocity to the magnetic field, i.e.

$$\varphi = \frac{|\alpha(\theta, \lambda) - \epsilon(\theta, \lambda)|_{\max}}{B} \tag{7}$$

Here, the φ values in different literatures are calculated respectively, as shown in Fig. 1(c). It can be found that the φ values in most of the other literatures are about 0.3 /T, while the φ value in this work can reach 2.92 /T, indicating a stronger sensitivity to the applied magnetic field. In addition, although the φ value of Ref. [21] is slightly higher than that of this work, its incidence angle is 65 °, which is far greater than the 1 ° achieved in this work.

Next, the influence of incident angle on nonreciprocal thermal radiation at resonant wavelength of 23.145 μm with $B = 0.3$T is discussed, as shown in Fig. 2(a) and (b). Firstly, as shown in Fig. 2(a), the absorptivity and emissivity spectra between 0° and 8° have been calculated. The results clearly show that the structure exhibits high emission levels close to 1 and low absorption near the incidence angle of 1° Moreover, as the incident angle increases to approximately 4°, the absorptivity can reach around 0.9, while the emissivity remains relatively lower at around 0.5. To further illustrate the variation of absorptivity and emissivity at the resonant wavelength with different incident angles, the corresponding angular distribution from 0° to 90° is calculated, as depicted in Fig. 2(b). It is evident that this structure not only exhibits a violation of Kirchhoff's law in the ultra-small angle range near 1° at the resonant wavelength but also demonstrates nonreciprocal thermal radiation phenomena over a larger angle range of 70–80° Here, in order to better show the nonreciprocity at the large angle, the absorptivity and emissivity spectra are calculated specifically for the peak angle of 73.05°, as depicted in Fig. 2(c). At the wavelength of 23.145 μm, the absorptivity reaches a value of 0.817, while the emissivity is only 0.269. Additionally, a relatively weak nonreciprocal thermal radiation is observed at 22.71 μm, with an emissivity of 0.781 and an absorptivity of 0.512. Therefore, as the incident angle increases, this structure also demonstrates a relatively weak dual-band nonreciprocal thermal radiation characteristic.

To further investigate the relationship between absorptivity and emissivity with the wavelength and incident angle, the corresponding dispersion relationships are calculated for two scenarios: $B = 0$T and $B = 0.3$T. The results are presented in Fig. 2(d, g) and (e, h), respectively. Firstly, when no external magnetic field is applied, it becomes evident that the absorptivity and emissivity are equal, indicating the absence of nonreciprocity. However, in contrast, when a magnetic field of 0.3T is applied, the absorptivity and emissivity spectra are no longer equal, which shows the violation of Kirchhoff's law. Here, in order to better show the nonreciprocity, the difference between the absorptivity and emissivity has been calculated varied with wavelength and incident angle, as shown in Fig. 2(f). The results demonstrate a pronounced nonreciprocity not only at ultra-small angles, specifically around 1°, but

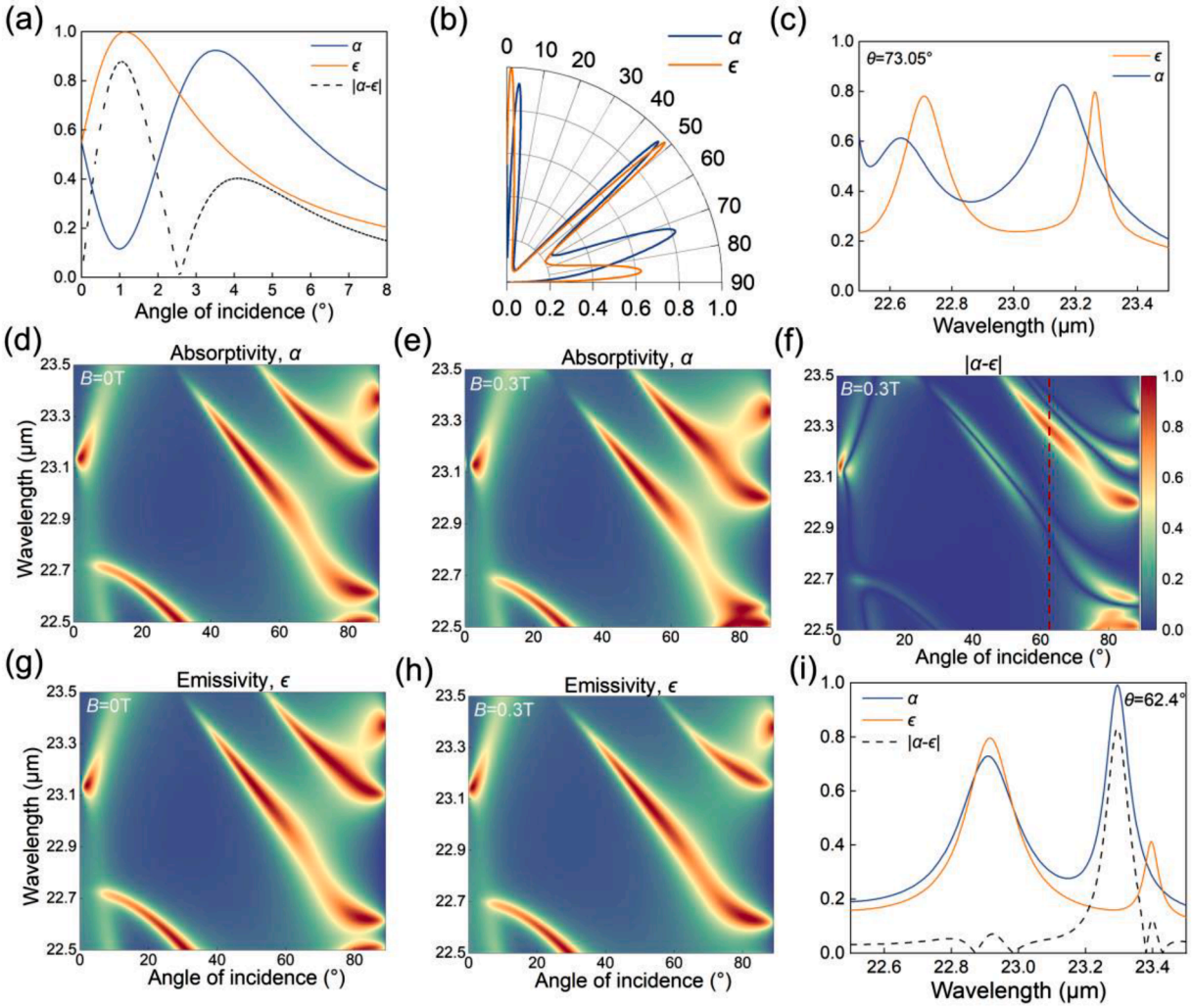

Fig. 2. Incident angle and wavelength dependences of nonreciprocal thermal radiation of MO structure. (a) The absorptivity and emissivity spectra between 0° and 8° for λ=23.145 μm with $B = 0.3$T. (b) Angular distribution diagram for λ=23.145 μm. (c) The absorptivity and emissivity spectra with $B = 0.3$T and θ=73.05° (d, g) The absorptivity and emissivity spectra vary with incident angle and wavelength with $B = 0$T, respectively. (e, h) The absorptivity and emissivity spectra vary with incident angle and wavelength with $B = 0.3$T, respectively. (f) The difference between absorptivity and emissivity varies with incident angle and wavelength with $B = 0.3$T. (i) The absorptivity and emissivity spectra with $B = 0.3$T and θ=62.4°

also within a wide range of larger angles exceeding 50°. To further explore the difference between absorptivity and emissivity at larger angles, an incidence angle of 62.4° is selected, corresponding to the red dotted line in Fig. 2(f), and the spectra are shown in Fig. 2(i). Remarkably, at a wavelength of 23.295 μm, the absorptivity reaches 0.993, while the emissivity is only 0.160, revealing that this structure can exhibit significant nonreciprocity even at large angles.

Considering that there is a small deviation during the fabrication, the values of the structural dimension parameters are changed by a deviation of ±5 %. The simulated results have been showed in Fig. 3(a)-(f) for different h_1, h_2, h_3, h_4, p and w, respectively. Firstly, as shown in Fig. 3 (a), no matter h_1 increases to 0.25 μm or decreases to 0.23 μm, the corresponding nonreciprocity, that is, the difference between the absorptivity and emissivity, basically coincides, indicating that h_1 has little influence on nonreciprocity within a deviation of ±5 %. Similarly, the fluctuation of parameters h_2 and h_4 within a deviation of ±5 % also has little effect on the nonreciprocal spectrum, and the peak position of the nonreciprocity remains centered around 23.145 μm, with a nonreciprocity value approaching 0.9, as shown in Fig. 3(b) and (d). As shown in Fig. 3(c), when the value of the parameter h_3 increases from 3.65 μm to 4.03 μm, the corresponding nonreciprocal spectrum is shifted from 22.85 to 23.44 μm, which shows a large redshift and the redshift distance is 0.59 μm. Besides, it can be clearly seen that the nonreciprocity remains close to 0.9. Similarly, the increase of parameters p and w will also lead to the redshift phenomenon of the nonreciprocal spectrum, as shown in Fig. 3(e) and (f). Therefore, the nonreciprocal spectra are insensitive to the parameters h_1, h_2 and h_4, but sensitive to h_3, p and w. In addition, it can be clearly seen that the changes of these parameters basically do not affect the nonreciprocity, demonstrating a very good stability of strong nonreciprocity.

In addition, controlling the directivity of the emitted thermal radiation is a challenge in contemporary photonic engineering. In this work, in addition to achieving nonreciprocal thermal radiation at very small angles, strong nonreciprocity can still be achieved at other angles by adjusting the thickness of h_2 while keeping other structural parameters unchanged. Fig. 4 respectively shows the difference of absorptivity and emissivity with h_2 at different incidence angles. It can be seen that strong nonreciprocity can still be achieved by adjusting the thickness of h_2 at different incident angles. For example, as shown in Fig. 4(c), the difference of absorptivity and emissivity can reach 0.91 at the wavelength of 23.95 μm with $\theta = 30°$ and h_2 =4.4 μm. Therefore, by adjusting the thickness of h_2, the nonreciprocal thermal radiation at different incident angles can be well realized to meet the application requirements of different scenarios.

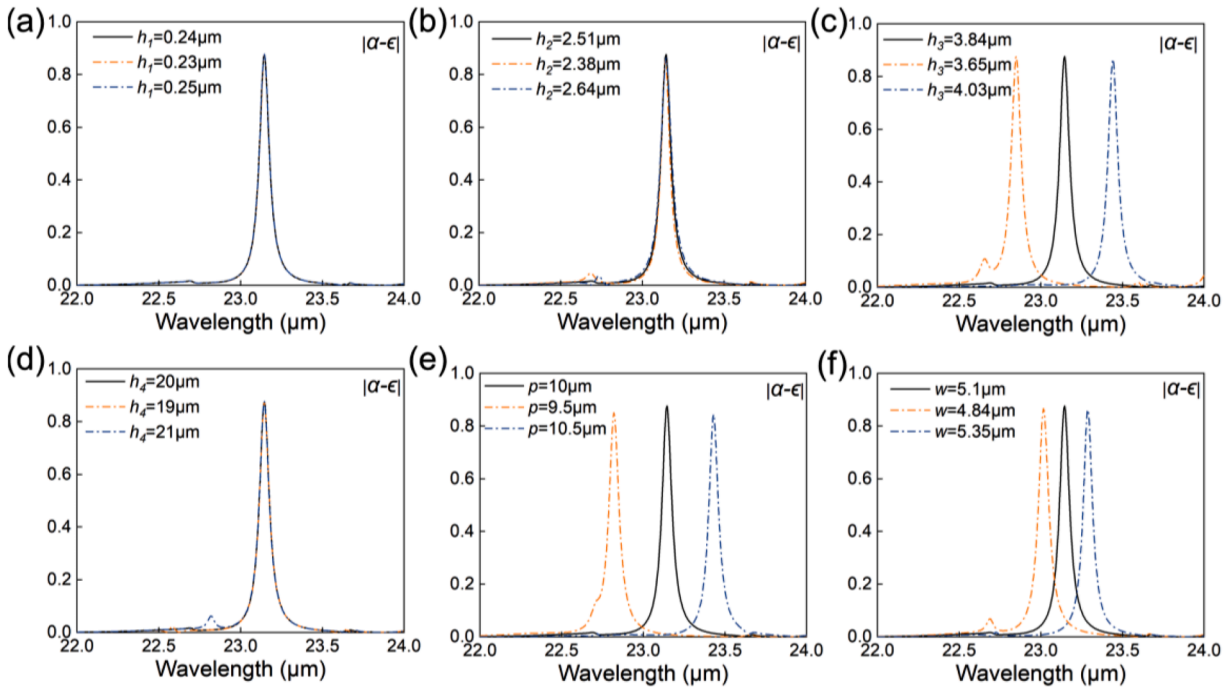

Fig. 3. Dependence of absorptivity and emissivity on different structure parameters: (a) h_1, (b) h_2, (c) h_3, (d) h_4, (e) p, (f) w.

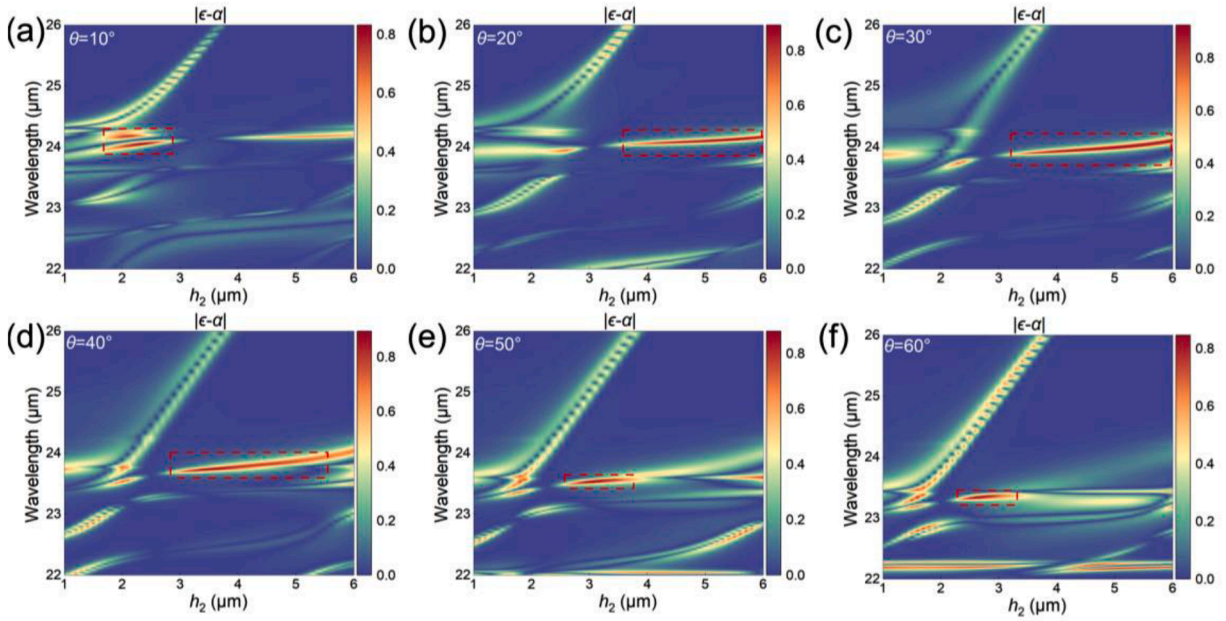

Fig. 4. Directional nonreciprocal thermal radiation of MO structure with $B = 0.3$ T. The difference of absorptivity and emissivity at different incident angles: (a) $\theta = 10°$, (b) $\theta = 20°$, (c) $\theta = 30°$, (d) $\theta = 40°$, (e) $\theta = 50°$, (f) $\theta = 60°$

Finally, considering the feasibility of this design, the bottom metal layer and the upper MO layer can be obtained by coating technology on the quartz plate. After that, the SiC film and metal Al film are coated on the above structure, and the grating structure is prepared by lithography or etching technology. In addition, since the magnetic field required for this design is only 0.3T, the external magnetic field can be provided with a permanent magnet on the market and other testing procedures can refer to Ref. [25].

4. Conclusions

In conclusion, in order to obtain a nonreciprocal thermal emitter with an ultra-small incident angle and moderate magnetic field, the structure of metal-SiC grating above on a MO film has been proposed, which realizes the strong nonreciprocity near the normal direction. This design is not only able to achieve a violation of Kirchhoff's law with θ=1°, but also exhibits the smaller magnetic field requirement compared to existing studies. The realization of this phenomenon is mainly due to the use of guided-mode resonance in the low-loss dielectric grating on MO materials, which greatly improves the sensitivity to the external

magnetic field. In addition, through an investigation into the impact of incident angles on the nonreciprocal spectrum, it has been discovered that this design not only achieves nonreciprocity at ultra-small angles but also exhibits substantial violation of Kirchhoff's law at larger angles (above 50°). These findings greatly enhance the angle selectivity for practical applications. What's more, the nonreciprocity maintains stability across a significant fluctuation range of structural dimension parameters, which can effectively reduce production costs. In addition, just by adjusting the thickness of h_2, not only the original nonreciprocal effect can be realized, but also the directional nonreciprocal thermal radiation can be realized. The present findings remove the limitations of large magnetic field and large incident angle for traditional nonreciprocal thermal radiation, and promote the practical realization and application of nonreciprocal thermal emitters.

CRediT authorship contribution statement

Zihe Chen: Writing – review & editing, Writing – original draft, Methodology, Investigation, Formal analysis, Conceptualization. **Shilv Yu:** Writing – review & editing, Investigation. **Cheng Yuan:** Writing – review & editing. **Xiaobing Luo:** Writing – review & editing. **Run Hu:** Writing – review & editing, Project administration, Funding acquisition, Conceptualization.

Declaration of competing interest

The authors declare that they have no known competing financial interests or personal relationships that could have appeared to influence the work reported in this paper.

Data availability

Data will be made available on request.

Acknowledgement

The authors would like to acknowledge the financial support by National Natural Science Foundation of China (52211540005, 52076087), Natural Science Foundation of Hubei Province (2023AFA072), the Open Project Program of Wuhan National Laboratory for Optoelectronics (2021WNLOKF004), Wuhan Knowledge Innovation Shuguang Program.

References

[1] G.I. Kirchhoff, On the relation between the radiating and absorbing powers of different bodies for light and heat, London, Edinburgh, Dublin Philos. Mag. J. Sci. 20 (1860) 1–21.
[2] Z. Zhang, X. Wu, C. Fu, Validity of Kirchhoff's law for semitransparent films made of anisotropic materials, J. Quant. Spectrosc. Radiat. Transf. 245 (2020) 106904.
[3] L. Zhu, S. Fan, Near-complete violation of detailed balance in thermal radiation, Physical Review B 90 (22) (2014) 220301.
[4] Y. Park, B. Zhao, S. Fan, Reaching the ultimate efficiency of solar energy harvesting with a nonreciprocal multijunction solar cell, Nano Lett. 22 (1) (2022) 448–452.
[5] S. Jafari Ghalekohneh, B. Zhao, Nonreciprocal Solar Thermophotovoltaics, Phys. Rev. Appl. 18 (3) (2022) 034083.
[6] Y. Park, Z. Omair, S. Fan, Nonreciprocal thermophotovoltaic systems, ACS Photonics 9 (12) (2022) 3943–3949.
[7] M.A. Green, Time-asymmetric photovoltaics, Nano Lett. 12 (11) (2012) 5985–5988.
[8] Z. Zhang, L. Zhu, Nonreciprocal thermal photonics for energy conversion and radiative heat transfer, Phys. Rev. Appl. 18 (2) (2022) 027001.
[9] C. Khandekar, F. Khosravi, Z. Li, Z. Jacob, New spin-resolved thermal radiation laws for nonreciprocal bianisotropic media, New J. Phys. 22 (12) (2020) 123005.
[10] B. Zhao, C. Guo, C.A.C. Garcia, P. Narang, S. Fan, Axion-Field-Enabled nonreciprocal thermal radiation in weyl semimetals, Nano Lett. 20 (3) (2020) 1923–1927.
[11] S. Pajovic, Y. Tsurimaki, X. Qian, G. Chen, Intrinsic nonreciprocal reflection and violation of Kirchhoff's law of radiation in planar type-I magnetic Weyl semimetal surfaces, Physical Review B 102 (16) (2020) 165417.
[12] Y. Tsurimaki, X. Qian, S. Pajovic, F. Han, M. Li, G. Chen, Large nonreciprocal absorption and emission of radiation in type-I Weyl semimetals with time reversal symmetry breaking, Physical Review B 101 (16) (2020) 165426.
[13] Z. Zhang, L. Zhu, Broadband nonreciprocal thermal emission, Phys. Rev. Appl. 19 (1) (2023) 014013.
[14] M. Liu, S. Xia, W. Wan, J. Qin, H. Li, C. Zhao, L. Bi, C.W. Qiu, Broadband mid-infrared non-reciprocal absorption using magnetized gradient epsilon-near-zero thin films, Nat. Mater. 22 (2023) 1196–1202.
[15] J. Wu, F. Wu, X. Wu, Strong dual-band nonreciprocal radiation based on a four-part periodic metal grating, Opt. Mater. 120 (2021) 111476.
[16] X. Wu, R. Liu, H. Yu, B. Wu, Strong nonreciprocal radiation in magnetophotonic crystals, J. Quant. Spectrosc. Radiat. Transf. 272 (2021) 107794.
[17] J. Wu, Z. Wang, B. Wu, Z. Shi, X. Wu, The giant enhancement of nonreciprocal radiation in Thue-morse aperiodic structures, Opt. Laser Technol. 152 (2022) 108138.
[18] J. Wu, F. Wu, T. Zhao, M. Antezza, X. Wu, Dual-band nonreciprocal thermal radiation by coupling optical Tamm states in magnetophotonic multilayers, Int. J. Therm. Sci. 175 (2022) 107457.
[19] Z. Chen, S. Yu, B. Hu, R. Hu, Multi-band and wide-angle nonreciprocal thermal radiation, Int. J. Heat Mass Transfer 209 (2023) 124149.
[20] Z. Chen, S. Yu, C. Yuan, K. Hu, R. Hu, Ultra-efficient machine learning design of nonreciprocal thermal absorber for arbitrary directional and spectral radiation, J. Appl. Phys. 134 (20) (2023) 203101.
[21] B. Zhao, Y. Shi, J. Wang, Z. Zhao, N. Zhao, S. Fan, Near-complete violation of Kirchhoff's law of thermal radiation with a 0.3 T magnetic field, Opt. Lett. 44 (17) (2019) 4203–4206.
[22] K. Shi, Y. Xing, Y. Sun, N. He, T. Guo, S. He, Thermal vertical emitter of ultra-high directionality achieved through nonreciprocal magneto-optical lattice resonances, Adv. Opt. Mater. 10 (24) (2022) 2201732.
[23] J. Wu, F. Wu, T. Zhao, X. Wu, Tunable nonreciprocal thermal emitter based on metal grating and graphene, Int. J. Therm. Sci. 172 (2022) 107316.
[24] J. Wu, Y.M. Qing, Near-perfect nonreciprocal radiation for extremely small incident angle based on cascaded grating structure, Int. J. Therm. Sci. 190 (2023) 108340.
[25] K.J. Shayegan, B. Zhao, Y. Kim, S. Fan, H.A. Atwater, Nonreciprocal infrared absorption via resonant magneto-optical coupling to InAs, Sci. Adv. 8 (2022) eabm4308.
[26] J. Wu, Y.M. Qing, The enhancement of nonreciprocal radiation for light near to normal incidence with double-layer grating, Adv. Compos. Hybrid Mater. 6 (3) (2023) 87.